We are IntechOpen,
the world's leading publisher of Open Access books
Built by scientists, for scientists

6,900
Open access books available

186,000
International authors and editors

200M
Downloads

Our authors are among the

154
Countries delivered to

TOP 1%
most cited scientists

12.2%
Contributors from top 500 universities

CLARIVATE ANALYTICS
BOOK CITATION INDEX
INDEXED

WEB OF SCIENCE™

Selection of our books indexed in the Book Citation Index
in Web of Science™ Core Collection (BKCI)

Interested in publishing with us?
Contact book.department@intechopen.com

Numbers displayed above are based on latest data collected.
For more information visit www.intechopen.com

Carbon-Based Nanocomposite Materials for High-Performance Supercapacitors

*Prasanta Kumar Sahoo, Chi-Ang Tseng, Yi-June Huang and Chuan-Pei Lee*

Abstract

Lightweight, flexible, wearable, and portable electronic gadgets have drawn significant attention in modern electronics industry. To power these gadgets, great efforts have been made to develop highly efficient energy-storage equipment. Among various power sources, a supercapacitor, acting as a bridge between the conventional battery and electrolytic capacitor, has been considered a promising portable energy storage device because of its high power density, fast charge/discharge rate, adequate operational safety, and excellent working lifetime. Hybrid supercapacitors, which combine redox materials with carbon-based materials, exhibit tremendous potential to fulfill the requirement of practical applications. In this chapter, we will review recent reports focusing on composite materials (*i.e.* metal oxide, metal hydroxide, and metal dichalcogenide composited with carbon materials) for the application in supercapacitors. The conclusion and futuristic prospects and challenges of highly efficient supercapacitors are briefly discussed.

Keywords: energy storage, composites, metal oxides, metal hydroxides, transition metal dichalcogenides, supercapacitor

1. Introduction

There is sharply increasing demand for energy with the rapid growth of the global economy. The energy generation from sustainable sources, such as wind and solar, plays an important role in power supply. However, the intermittent nature and imbalanced regional distribution of the sustainable energy make them unable to stably supply the power [1]. The development of energy storage systems is an urgent requirement to meet the sufficient and stable power supply for industrial and residential usage. Although rechargeable lithium-ion batteries, dominant energy sources in each field, as high energy density providers have filled their position [2], lithium-ion batteries still have the limitations of poor cycle life and low power performance [3]. Supercapacitors (SCs), also known as ultracapacitor and electro-chemical capacitors, are an emerging class of energy storage device, which possess high power density and tens of thousands of charge/discharge cycles [4, 5]. **Figure 1** shows the Ragone plot of different energy conversion and storage devices. SCs have a unique position to bridge the gap between conventional capacitors and batteries. Compared with conventional capacitor, SCs possess higher specific energy density
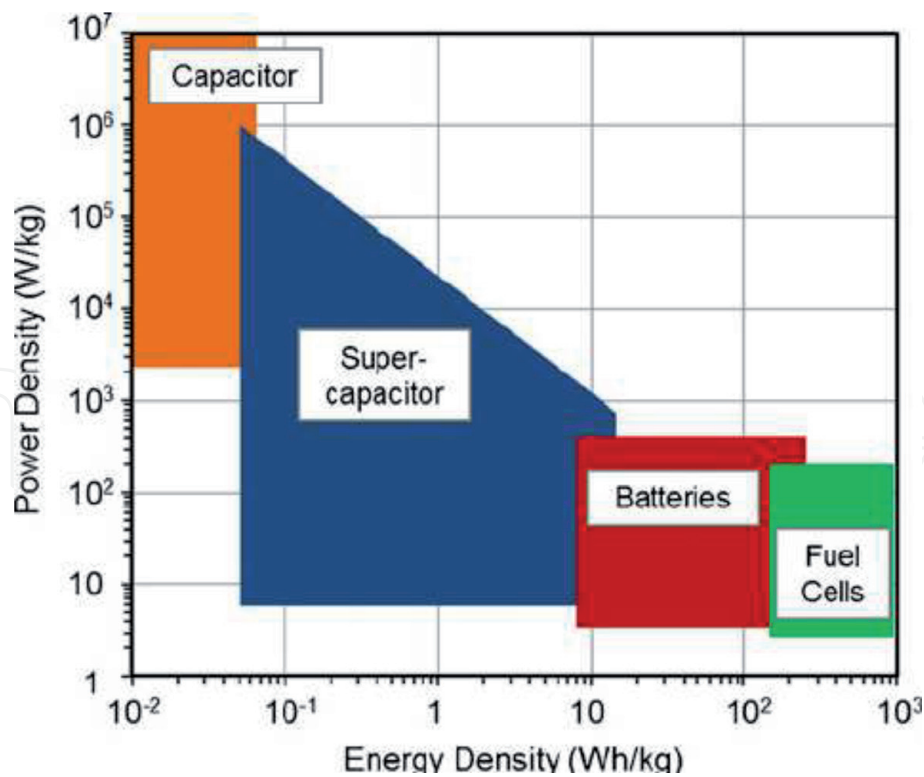
Figure 1.
Ragone plot for various energy storage and conversion devices [6].

in several orders of magnitude. Moreover, SCs provide higher specific power density than batteries due to its unique charge storage mechanism.

2. Theoretical background for supercapacitors

2.1 Principle and mechanism of supercapacitors

Based on different charge storage mechanisms, SCs are mainly divided into two categories, electrical double layer capacitors (EDLCs) and pseudocapacitors, as shown in **Figure 2**. EDLCs store the electrical charge by electrostatic force at the electrode-electrolyte interface, which is a physical process without involving electrochemical reactions on the electrode surface. In order to increase the capacitance and energy density of SCs, some electrochemically active materials, such as transition metal oxide and conducting polymers, have been explored as electrode materials for pseudocapacitors. The energy storage in pseudocapacitors originates from reversible surface faradaic redox reactions at the interface of electrolyte and electroactive materials.

2.2 Factors affecting the performance of Supercapacitors

The capacitance of EDLCs is strongly dependent on effective surface area and the pore size distribution of the electrode [7, 8]. Typically, the carbon-based materials and their derivatives, including activated carbon, carbon nanotubes (CNTs) and graphene, with high conductivity, chemically-stability, and large surface area are widely utilized in EDLCs. Although the EDLCs possess high power density and excellent charge/discharge cycling stability, they suffer from low energy density owing to the relatively low capacitance of carbon-based materials. Pseudocapacitors

can achieve significantly higher energy density, as compared to EDLCs, because they have a variety of oxidation states for redox charge transfer reactions. However, relatively low electrical conductivity and poor rate capability and cycle stability of pseudocapacitive materials limit their widespread commercial applications [9]. Therefore, carbon-based materials with high conductivity and distinct structures can be combined with pesudocapacitive materials to exhibit synergistic effects for supercapacitive performance, known as hybrid SCs.

## 3. Carbon based composite electrode materials

Carbon material is EDLCs type for supercapacitor. In section 2.1, EDLCs has introduced their property, which store the electrical charge by electrostatic force at the electrode-electrolyte interface, as shown in **Figure 2**. It is not involving electrochemical reactions on the electrode surface. There are different types of carbon nanostructured materials, which can be used as single electrode materials due to their unique structural, mechanical, and electrical properties.
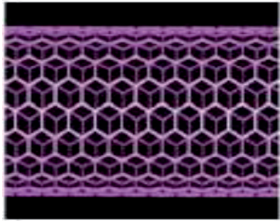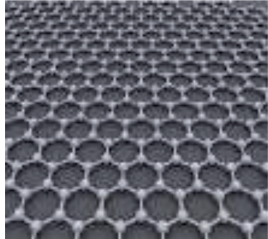
3.1 Zero-dimensional (0-D) carbon nanoparticles

They are round-shaped particles such as ultrafine activated carbon (AC), mesoporous carbon, carbon nanosphere, and carbon quantum dot, with a high specific area (AC: ~3000 $m^2\,g^{-1}$) and an aspect ratio of nearly [10]. In addition, by tuning the pore size distribution and pore content, they can use as suitable supporting materials for composite electrodes.

3.2 One-dimensional (1-D) carbon nanostructures

These are the high aspect ratio materials with fiber shaped and good electronic properties e.g. carbon nanotubes (CNT), carbon nanocoils, and carbon nanofibers (CNF), which facilitates the electrochemical reaction kinetics by 1-D charge transfer pathway.
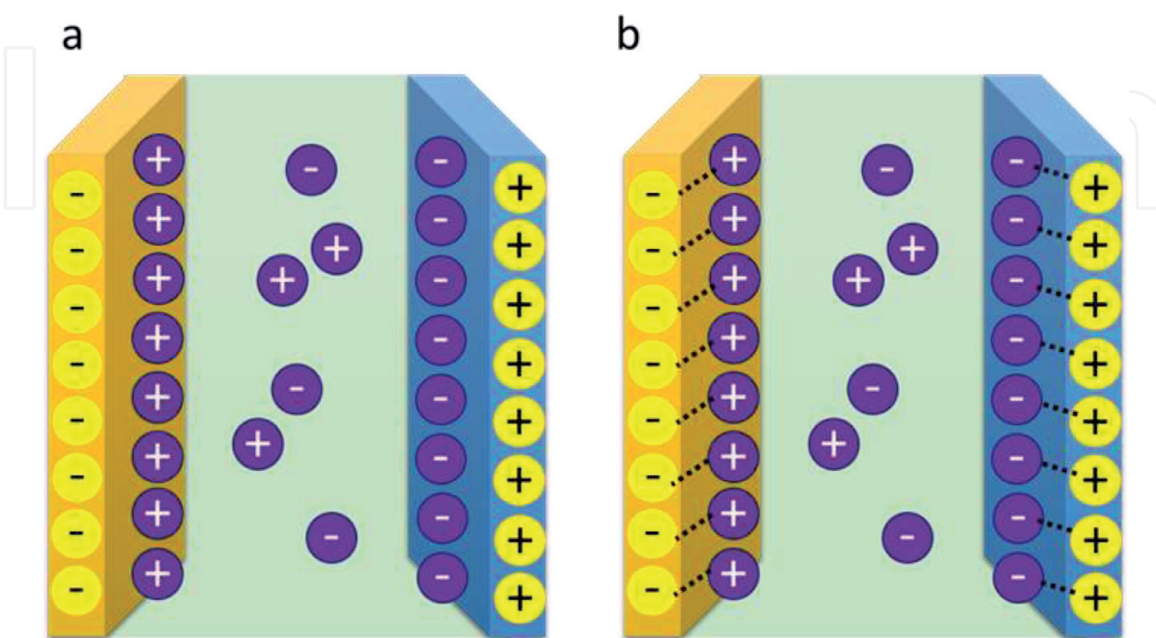
Figure 2.
Schematic diagram of (a) an electrical double layer capacitor and (b) a pseudocapacitor.

Materials	Carbon onions	Carbon nanotubes	Graphene	Templated carbon
Dimensionality	0D	1D	2D	3D
Conductivity	High	High	High	Low
Volumetric Capacitance	Low	Low	Moderate	Low
Cost	High	High	Moderate	High
Structure				

Table 1.
Different carbon nanostructures used as electrode materials for EDLCs with onion-like carbon, carbon nanotubes, graphene, activated carbon, carbide-derived carbon, and templated carbon [16].

3.3 Two-dimensional (2-D) nanosheets

They are sheet like structures with high aspect ratio such as graphene, graphene oxide (GO) or reduced graphene oxide (rGO). In addition, they have high specific surface area, good mechanical strength, and excellent electrotonic conductivity, which helps them as promising electrode materials for SCs. For an example, single layered graphene has theoretical surface area of 2756 $m^2\,g^{-1}$ and charge mobility of 200000 $cm^2\,V^{-1}\,s^{-1}$ [11].

3.4 Three-dimensional (3-D) porous nanostructures

These are the low dimensional building blocks such as carbon nanofoams or sponges with hierarchical porous channels, rich pore structures, higher electrical conductivity and better structural mechanical stability, which are extensively used in composite electrode materials for SCs. For an example, foam has high specific surface area with continuous electron transport path and large area of electrolyte-electrode interface.

Table 1 shows some examples of different carbon nanostructured materials such as carbon onions, carbon nanotubes, graphene, and templated carbon, which are used as electrode materials for EDLCs. Each carbon nanostructured materials have its advantages and disadvantages. For example, carbon onions have high power performance due to excellent conductivity with high accessible ion adsorption capacity but low capacitance of ~30 $F\,g^{-1}$ [12]. On the other hand, CNTs have high energy density due to superior electrical properties and unique tubular structures for fast charge transportation but due to the high cost, their widespread applications are limited [13]. Recently, graphene has been attracted much attention as electrode materials for EDLC applications due to unique properties, like as ultrahigh specific surface area, unique conductivity, and exceptionally high mechanical strength [14]. However, the aggregation of sheets during electrode preparation limits the aspect of application. More recently, 3D porous carbon nanostructured materials are widely used for EDLCs because of rich pore structures and high surface areas but due to relative low conductivity and presence of micropores specific capacitance is insufficient at a high current density [15]. Therefore, it is necessary to construct composite materials by coupling the advantages of different types of carbon nanostructured materials and high energy electrode materials such as transition metal oxides, metal hydroxides and metal dichalcogenides (TMDs) to enhance the energy density without the compromise of power density and also meet the requirement for fabrication of high energy storage devices. In the composite electrode material, different types of carbon nanostructured materials not only contribute to high capacitance but also provide an easy conductive path for charge transportation due to conductive nature.

4. Carbon-metal oxide composite electrode materials

Many metal oxide such as RuO_2, MnO_2, Fe_3O_4, V_2O_5, NiO, Co_3O_4, and TiO_2, has been received significant attention and extensive studied as SC electrode materials due to Pseudo capacitance nature, which depends on the fast reversible redox reaction of electroactive species directly as well as in the vicinity of electrode surface [17–20]. The redox behavior is due to the multivalent property of the above oxides which changes their oxidation states by interaction with protons or hydroxide ions reversibly. In spite of their excellent specific capacitance, they still suffer from low conductivity, low rate capability, poor stability and durability during the process of charge/discharge. In contrast carbon materials shows excellent performance in

these regards but suffer from comparatively limited specific capacitance. Hence, the synergic integration of metal oxides with conducting carbon supports may form high potential carbon-metal oxide composite electrodes materials for SCs and hybrid devices because of their enhanced electrochemical performance through the combined effect of pseudocapacitive/faradaic charge storage and electrical double layer capacitance mechanisms [21–23].

4.1 Carbon-ruthenium oxide (RuO_2)-based composite electrode materials

Among the metal oxides, ruthenium oxide (RuO_2) has been considered as very common electrode materials for SCs in acidic medium due to their excellent pseudocapacity which is arising from high conductivity, good thermal stability, highly reversible redox reactions, three different oxidation states within 1.2 V, and high specific capacitance natures. The pseudocapacitance mechanism of RuO_2 for SC electrodes can be described as equation [24]:

$$RuO_2 + xH^+ + xe^- = RuO_{2-x}(OH)_x \ (0 \leq x \leq 2) \tag{1}$$

Or

$$RuO_2 + H^+ + e^- = RuOOH \tag{2}$$
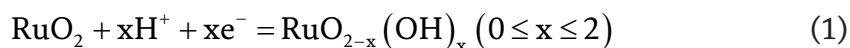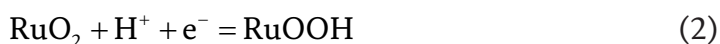
However, its scarcity and high cost limits the fabrication of RuO_2 based electrodes for potential applications. But, smartly use of composite materials by synergic integration of pseudocapacitive RuO_2 materials with conductive carbonaceous substrates not only improves the capacitance but also reduces the cost of the electrode. Recent studies are more focus about the selecting the best carbonaceous substrate and the synthesis procedures to fabricate ruthenium oxide (RuO_2)-coated on the porous carbonaceous substrates.

RuO_2-CNT composite has been prepared by uniformly coating of RuO_2 on the vertically aligned porous carbon nanotubes porous through atomic layer deposition (ALD) technique and further activation by voltammetry potential coulometry (**Figure 3(a-c)**) [25]. This ALD technique has many advantages such as deposition on large surface area, accurate thickness and exceptional uniformity for electrode designing in energy storage devises. The as-prepared RuO_2-CNT composite shows excellent electrochemical performance as an electrode material for SC in respect of capacitance, power density and stability. Several publications have been reported the specific capacitance and power density of RuO_2-CNT composite, which are around 650 F g^{-1} and 17 kW kg^{-1}, respectively. Kaner *et.al* recently demonstrated the synthesis and processing of 3D porous RuO_2/laser-scribed graphene (LSG) composite electrode for miniaturized and interdigitated SC that exhibit ultrahigh energy and power density (**Figure 3(d)**) [26]. The high-resolution TEM (HRTEM) image of 3D porous RuO_2/LSG composite in **Figure 3(e)** shows that multiple layers of the graphene sheets wrap around each RuO_2 nanoparticle. 3D porous RuO_2/LSG composite electrode showed an ultrahigh specific capacitance of 1139 Fg^{-1} with outstanding rate capability and the asymmetric supercapacitor (ASC) made of 3D porous RuO_2/LSG composite electrode as positive electrode exhibited an extremely high energy density of 55 W h kg^{-1} at a power density of 12 kW kg^{-1} (**Figure 3(f)**). Other interesting composite of RuO_2 made of RuO_2 decorated nitrogen-doped reduced graphene oxide aerogel (NGA) are used as high-performance transparent
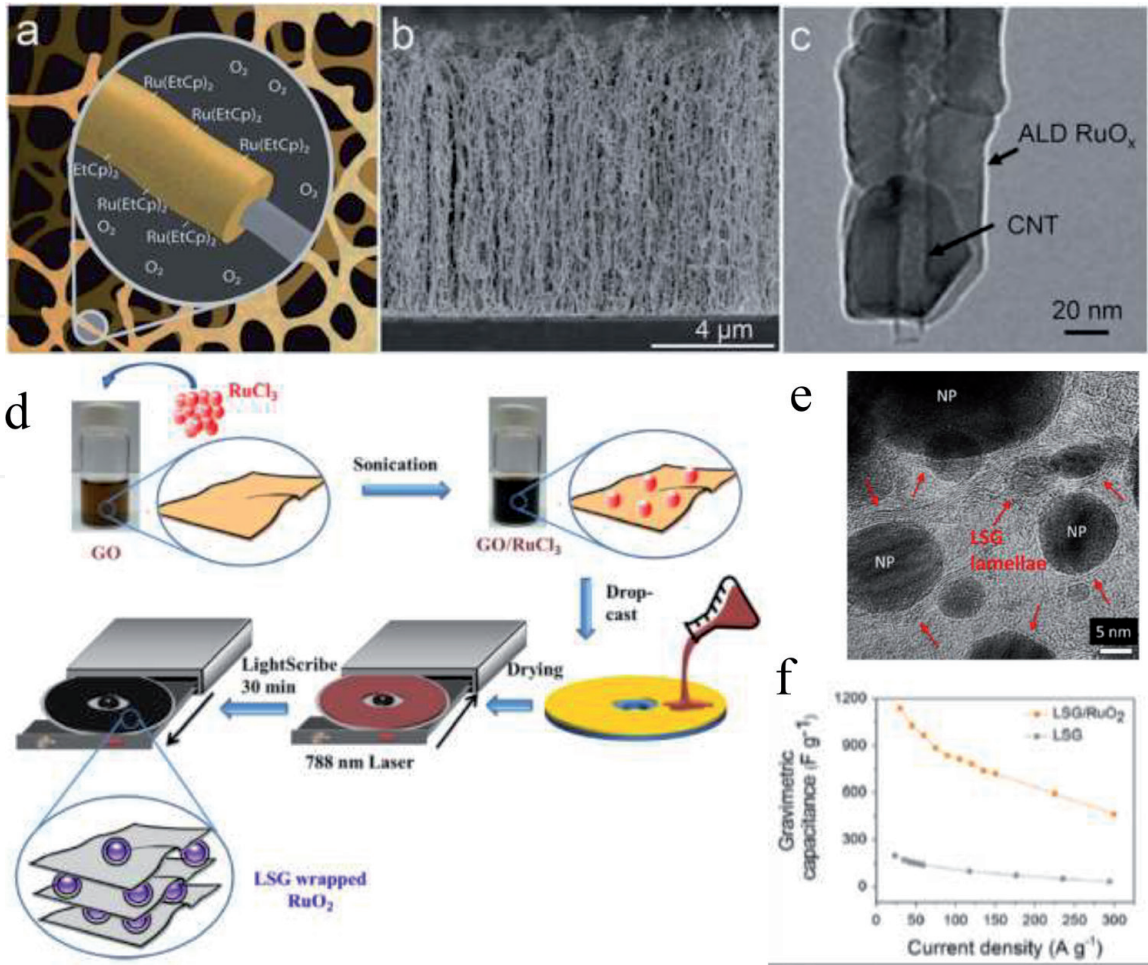
Figure 3
(a) Schematic presentation of RuO_x deposited on the vertically aligned porous carbon nanotubes porous through ALD by sequential pulsing of Ru $(EtCp)_2$ and oxygen. (b) and (c) SEM and TEM images of vertically aligned CNTs coated with ALD RuO_x [25]. (d) Microfabrication process of 3D porous RuO_2/LSG interdigitated micro-supercapacitors through direct laser writing on a DVD disc using a LightScribe DVD burner. (e) A high-magnification TEM image of 3D porous RuO_2/LSG composite showing complete wrapping of the RuO_2 nanoparticles (NP) by multiple layers of the graphene sheets. (f) The gravimetric capacitance retention of laser scribed graphene (LSG) and RuO_2/LSG electrodes as a function of the applied current density [26].

solid-state supercapacitors. RuO_2/NGA composite with finely tuned mass loading of 16.3 µg cm^{-2} and transmittance of 34.1% (λ = 550 nm) demonstrated maximum areal energy of 0.074 µW h cm^{-2} and power of 64 µW cm^{-2} with cyclic stability of 100% over 2000 cycles [27]. This RuO_2/NGA based high transparent SC can be practically used in many advanced transparent electrical devices.

4.2 Carbon-manganese oxides (MnO_2)-based composite electrode materials

MnO_2 has been considered as a promising pseudocapacitive electrode materials for energy storage applications due to low price, abundant reserve, high specific capacitance, and environmental environment benign nature and low toxicity in comparison to other transition-metal oxides. In general, the charge storage mechanism of MnO_2 involves change in manganese oxidation state from +3 to +4 and the contribution of protons or alkali cations, which can be shown in the following equation [28].

$$MnO_2 + C^+ + e^- \leftrightarrow MnOOC \qquad (3)$$

Where C^+ represents protons or alkali cations (Li^+, Na^+, K^+).

However, MnO_2 based electrodes limits the capacity and power density due to their low surface area and poor electronic/ionic conductivity. Therefore, the composite of MnO_2 with high-surface area and conducting carbonaceous materials may improve the electrochemical performance in terms of specific capacity, energy and power densities by providing the larger interfacial area between the MnO_2 particles and the electrolyte solution [29].

Gao *et al.* fabricated a MnO_2/activated carbon (AC) based hybrid SC, where AC not only acted as a conducting support but also increase the capacitance as well as energy and power densities [30]. In addition, engineering the morphology of MnO_2 into different nanostructures is considered to be a practical approach to increase its electrochemical performance. It is reported that the pore sizes of the mesoporous-MnO_2/AC are greatly affected the specific capacitance and the rate capability of the SCs. Huang *et al.* demonstrated the influence of CNT on the electrochemical properties of MnO_2-CNT composite electrode by controlling the growth of MnO_2 nanostructures on CNTs through a facile redox approach (**Figure 4(a-c)**) [31]. The as-prepared MnO_2-CNT composite electrode showed a maximum specific capacitance of 247.9 F g^{-1} with outstanding cyclic stability of 92.8% after 5000 cycles. In addition, it has been noticed that the aligned CNTs are more favoured as SC electrodes over nonaligned CNTs due to their large specific surface area, low contact resistance, and fast electron-transfer kinetics. Graphene is being used as a supporting material for MnO_2 nanostructures due to its large surface area, high conductivity, and high stability nature. For example, microwave
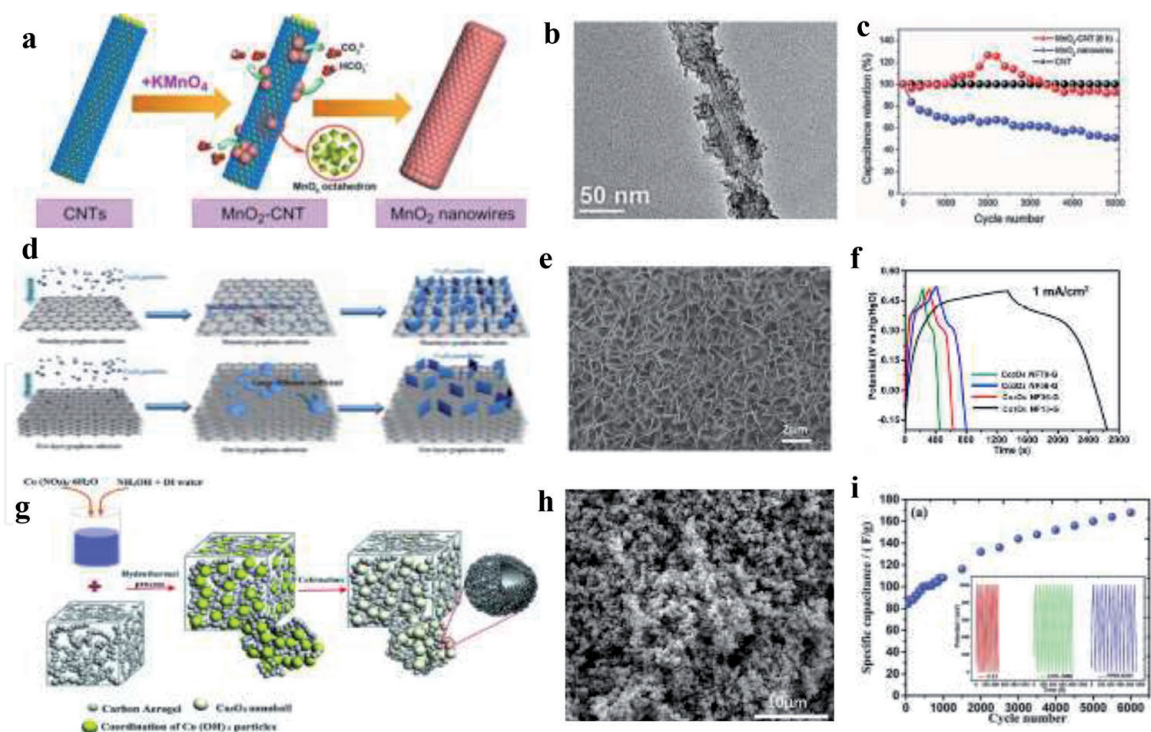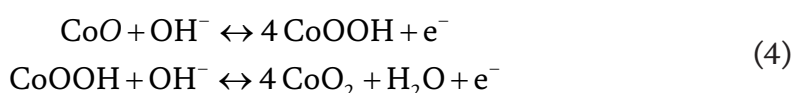

Figure 4.
(a) Controlled growth of MnO_2 nanostructured on CNT surface through facile redox method. (b) TEM images displaying coverage of MnO_2 on the surface of CNT. (c) The cyclic curve of a MnO_2-CNT nanowire composite at current density of 2 A g^{-1} [31]. (d) Schematic illustration of fabrication of Co_3O_4 nanoflake/graphene@ Ni hybrid electrode materials by in situ synthesis method. (e) Top-view SEM images of the Co_3O_4 nanoflake/ graphene/Ni hybrid electrode. (f) GCD curves of Co_3O_4 nanoflake/graphene/Ni hybrid electrode at current density of 1 mA cm^{-2} [39]. (g) A schematic of the synthesis of the porous Co_3O_4 nanoball/CA hybrid. (h) FE-SEM images of the porous Co_3O_4 nanoball/CA hybrid. (i) The specific capacitance test of the porous Co_3O_4 nanoball/CA hybrid electrode at a current density of 1 A g^{-1} as a function of cycle number (inset: 11 cycles continuous GCD curves obtained for porous Co_3O_4 nanoball/CA hybrid electrode for the different cycle numbers) [41].

irradiation synthesised MnO_2-graphene composites exhibited the maximum capacitance of 310 F g^{-1}, which is much higher than the bare graphene and MnO_2 (110 F g^{-1}) [32]. Beside their high capacitance, MnO_2-graphene composites have better cyclic stability of 95% over 15000 cycles. The excellent electrochemical performance of MnO_2-graphene composites is due to large surface area and high conductivity of graphene network. Recently, Zhang *et al.* reported highly flexible ASCs based on graphene hydrogel (GH)/copper wire (CW) as the negative electrode and hierarchical MnO_2/graphene/carbon fiber (CF) as the positive electrode, which exhibited excellent areal energy density of 18.1 μW h cm^{-2} and operated reversibly at potential window of 0-1.6 V [33]. 3D porous carbon nanostructures can also be used as MnO_2 support for supercapacitor (SC) electrodes as they provided large surface area, well-defined pathways to electrolyte access, and better mechanical stability. Fang *et al.* demonstrated a novel solid-state symmetric supercapacitor (SSC) based on 3D rGO@MnO_2 foam electrode and Polyacrylic Acid (PAA)-Portland cement-KOH electrolyte, which showed a very high areal capacity of 1.84 F cm^{-2} at current density of 0.5 mA cm^{-2} and excellent capacitance retention of 61% at a current density of 40 mA cm^{-2} [34].
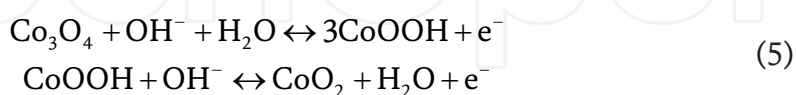
4.3 Carbon-cobalt oxides (CoO/Co_3O_4)-based composite electrode materials

Cobalt oxides has been received considerable attention as highly promising SC electrode materials due to their non-toxic, low cost, easy synthesis, environmentally friendly, and more importantly high theoretical capacitance (CoO: 4292 F g^{-1}, Co_3O_4: 3560 F g^{-1}) [35]. In addition, cobalt oxides exhibits outstanding electrochemical behaviour in alkaline as well as organic electrolyte, which is possible due to their ability to interact with the ions at the electrolyte surface as well as through the bulk of the material. The pseudocapacitance of cobalt oxides (CoO/Co_3O_4) are originates from the following redox reaction: [36]

CoO:

$$CoO + OH^- \leftrightarrow 4\,CoOOH + e^-$$
$$CoOOH + OH^- \leftrightarrow 4\,CoO_2 + H_2O + e^-$$

$\qquad\qquad\qquad\qquad\qquad\qquad\qquad\qquad\qquad\qquad\qquad (4)$

Co_3O_4:

$$Co_3O_4 + OH^- + H_2O \leftrightarrow 3CoOOH + e^-$$
$$CoOOH + OH^- \leftrightarrow CoO_2 + H_2O + e^-$$

$\qquad\qquad\qquad\qquad\qquad\qquad\qquad\qquad\qquad\qquad\qquad (5)$

However, the low electrical/ionic conductivity of cobalt oxides hinders their practical performance as SC electrodes. Most efficient way to improve their electrochemical performance is to form composites of cobalt oxides by incorporation into a carbon-based conducting supports. A Co_3O_4/AC composite SC electrode was reported by Iqbal *et al*. [37]. The electrode exhibited maximum achievable specific capacitance 567 F g^{-1} and maximum energy density of 63 W h kg^{-1} at 0.7 A g^{-1}. In addition to the high specific capacitance, Co_3O_4/AC composite of capacitive retentivity is 82% after 6000 charge/discharge cycles and safe to handle due to no leakage. The specific capacitance of the cobalt oxide strongly depends on the microstructure and morphology of the materials, which facilitate the electrolyte ion transport through the material more effectively. Sun *et al.* demonstrated a

simple and effective approach to grow well-aligned 3D cobalt oxide nanowire arrays (Co_3O_4 NWAs) directly on carbon nanotube fibers (CNTFs) through CVD process [38]. The Co_3O_4 NWAs/CNFs showed a specific capacitance of 734.25 F cm^{-3} (2210 mF cm^{-2}) at 1.0 A cm^{-3} and a high energy density of 13.2 mW h cm^{-3} at a current density of 1.0 A cm^{-3}. Graphene along with cobalt oxides can be used as a composite material for SCs because of its high conductivity, high surface area, high carrier mobility, and excellent mechanical strength. For example, an in situ synthesised Co_3O_4/graphene@NF hybrid composite electrode with a thickness of 13 nm exhibited a high specific capacitance of 1.75 F cm^{-2} at 1 mA cm^{-2} and a capacitance increase of 12.2% after 5000 cycles at 10 mA cm^{-2} (**Figure 4(d-f)**) [39]. Tseng *et al.* demonstrate a binder-free and flexible SC based on CoO/graphene hollow nanoballs (GHBs) composite electrode [40]. The as fabricated CoO/GHBs composite electrode exhibits high specific capacitance of 2238 F g^{-1} at a current density of 1 A g^{-1} and good rate capability of 1170 F g^{-1} at a current density of 15 A g^{-1}. The excellent capacitive performance and high rate capability were accomplished by the synergistic combination of conductive GHBs with large surface areas and highly pseudocapacitive CoO. In addition, as fabricated SSC demonstrated a very high power density (6000 W kg^{-1} at 8.2 W h kg^{-1}), high energy density (16 W h kg^{-1} at 800 W kg^{-1}), good cycling stability (~100% capacitance retention after 5000 cycles), and excellent mechanical flexibility at various bending positions. Recently, 3D-carbon aerogels (3D-CA) with appropriate electrical conductivity, high specific surface area and rich dielectric electrochemical stability when combined with the porous cobalt oxides can enabled the fabrication of an composite electrode with outstanding electrochemical performance.Co_3O_4/CA composite electrode which was synthesized through in situ growth method showed a specific capacitance of 350 F g^{-1} at 1 A g^{-1} and Energy density of 23.82 kW kg^{-1} at a power density of 95.96 W kg^{-1} (**Figure 4(g-i)**) [41]. The as-prepared ASC device could be cycled reversibly in a potential range of 0.0 to 1 V at 1 A g^{-1} and showed a capacity retention of 210% over 6000 cycles. Zhu *et al.* adopted a facile hydrothermal method to synthesize self-assembled cobalt oxide (CoO) nanorod cluster on 3D-graphene foam (CoO-3DGF) which exhibits a very high performance compared with CoO nanorod clusters grown on Ni foam (680 F g^{-1}) in terms of specific capacitance 980 F g^{-1} at 1 A g^{-1} and cycling stability of 103% over 10,000 cycles [42].

4.4 Carbon-binary metal oxide based composite electrode materials

Recently, binary metal oxides such as $NiCo_2O_4$, $NiFe_2O_4$, $CoFe_2O_4$, $ZnMnO_4$, and $ZnCo_2O_4$ have attracted much attention due to higher electrical conductivity than individual metal oxide and provide higher capacitance due to more affluent redox reaction than individual components [43]. Even though binary meal oxides possess better electrochemical performance than individual metal oxide extremely, they still suffer from inferior rate performance, low utilization rate and poor cycle stability. However, by incorporating carbon based materials improve their conductivity as well as power density due to high surface area, high conductivity and stable chemical properties of carbon based materials [44]. Kumar *et al.* fabricated Carbon black (CB) decorated Ni/Co oxide composite electrode through by using the successive ionic layer adsorption and reaction (SILAR) method [45]. Carbon black (CB) decorated Ni/Co oxide composite electrode with 7% weight percentage of CB exhibited a high specific capacitance of 1811 F g^{-1} at 0.5 mA cm^{-2} with excellent cyclic retention of 92% over 8000 cycles and delivered an impressive high energy density of 91 W h Kg^{-1} at a power density of 151 W Kg^{-1}, which is significantly higher than pure Ni/Co oxide composite electrode as well as other carbon embedded composites. Veerasubramani *et al.* have adopted a novel approach to fabricate

CNT-deposited $CoMoO_4$/Ni foam through a hydrothermal method followed by dry reforming reaction (DRR) of propane and CO_2 [46, 47]. The as fabricated CNT-deposited $CoMoO_4$/Ni foam electrode achieved a maximum areal capacity of 160 $\mu Ah\ cm^{-2}$ at 1 mA cm^{-2} with excellent cyclic stability of ~105% over 3000 cycles and showed 22-fold higher performance than the heat-treated $CoMoO_4$/Ni foam. The high electrochemical performance is due to the presence of CNTs on the surface of $CoMoO_4$/Ni foam electrode, which increases the conductivity of the electrode and enhances the ion transport kinetics. Further as fabricated ASC device, consists of CNT-deposited $CoMoO_4$/Ni foam as the positive electrode and reduced graphene oxide (rGO)-coated carbon cloth (CC) as the negative electrode stored a maximum areal energy density of 122 $\mu Wh\ cm^{-2}$ (29.04 Wh kg^{-1}) at 2 mA cm^{-2} and delivered a high power density of 7,727 μWcm^{-2} (1835 W kg^{-1}) 10 mA cm^{-2} with excellent capacitance retention of more than 95% of its initial capacitance over 1500 cycles. Soam *et al.* synthesized porous type of $NiFe_2O_4$/graphene nanocomposite electrode by a solution based process for supercapacitor application [48]. The as-prepared $NiFe_2O_4$/graphene nanocomposite electrode exhibited a maximum specific capacitance of 207 Fg^{-1} at a scan rate of 5 mV/sec, which is almost 4 times larger than pure $NiFe_2O_4$ (60 Fg^{-1}) and showed the capacitance retention of 95% over 1000 cycles. The significantly enhanced specific capacitance of the $NiFe_2O_4$/graphene nano-composite electrode material is due to the synergic effect of high porous graphene sheets and $NiFe_2O_4$ particles, which are strongly interconnected together leading to a good electric/ionic conduction on the electrode and better contact of ions with the electrode materials. Zhou *et al.* reported a novel and green Cu_2O template-assisted route based on "coordinating etching and precipitating" process for the synthesis of 3D porous reduced graphene (rGN)/$NiCo_2O_4$ film [49]. The as-synthesized 3D rGN/$NiCo_2O_4$ film exhibited high specific capacitance of 708.36 F g^{-1} at a current density of 1 A g^{-1} with a rate retention of 82.2% as current density ranges from 1 to 16 Ag^{-1}, and remarkable capacitance retention of 94.3% after 6000 cycles at a high current density of 10 A g^{-1}.

5. Carbon-metal hydroxide composites electrode materials

Among the active materials, metal hydroxides have also been considered promising electrode materials for electrochemical SCs because of extremely high specific capacitance. Metal hydroxide in several forms such as $Ni(OH)_2$, $Co(OH)_2$, $NiCo(OH)_2$, $Cu(OH)_2$, FeOOH have been investigated as electrodes for SC [50–52]. These materials have large internal spaces for fast insertion and desertion of electrolyte ions. Moreover, these metal hydroxides can be synthesized using simple synthetic approaches. Metal hydroxide consists of stacked layers intercalated having interlayer space to occupy more ions hence larger capacitance.

5.1 Carbon-nickel hydroxide ($Ni(OH)_2$) composite electrode materials

$Ni(OH)_2$ is being considered as an attractive candidate as electrode in SCs because of its high theoretical capacitance (2358 F g^{-1}). It can be prepared by a simple and low cost process. It has demonstrated good stability in alkaline electrolytes. Its low electrical conductivity is a barrier to achieve higher capacitance. Therefore, a thin region near the surface of nickel hydroxide contributes to the charge storage process due to diffusion-limited redox reactions. To obtain larger capacitance, it has to be utilized completely in the charge storage process. In this regard, researchers have generally adopted conductive additives to effectively improve utilization of active materials and result in larger capacitance. Kang *et al.* have used the same concept
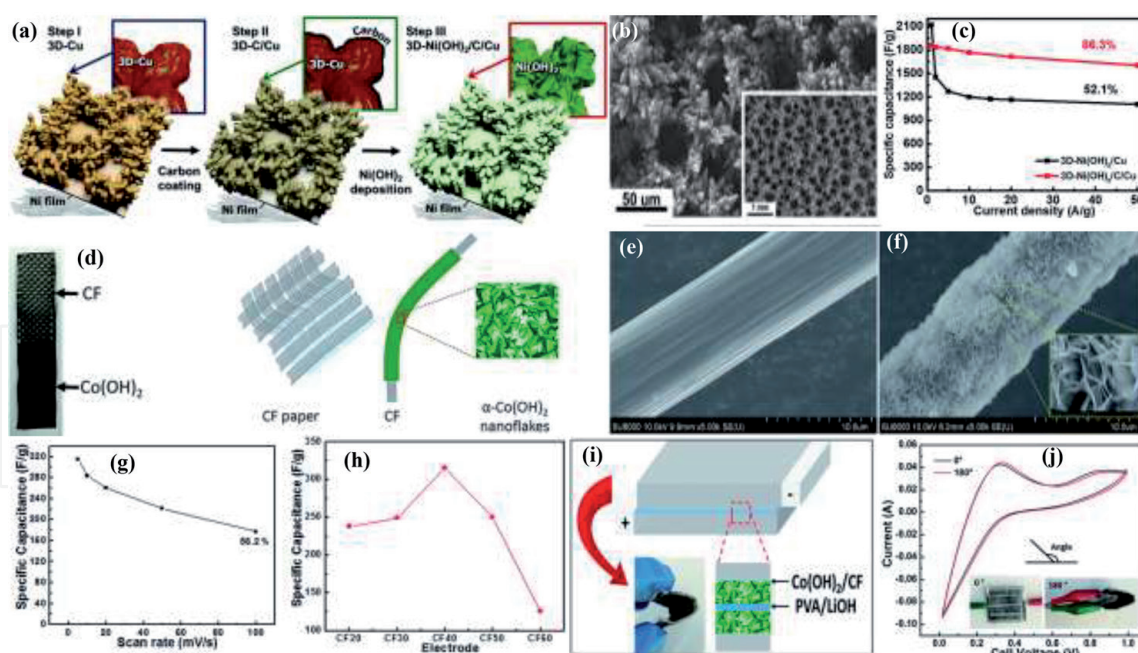
Figure 5.
(a) A schematic of the growth process of 3D-Ni(OH)₂/C/Cu, (b) Morphology of the as-synthesized 3D-Ni(OH)₂/C/Cu electrode (inset: large-area uniform porous morphology of the 3D-Ni(OH)₂/C/Cu), (c) Specific capacitance of 3DNi(OH)₂/C and 3D-Ni(OH)₂/C/Cu as a function of the current density based on the galvanostatic charge/discharge measurement [53], (d) Photograph of CF paper coated with cobalt hydroxide nanoflakes and schematic diagram illustrating the loading procedure of cobalt hydroxide on CF, (e) SEM image of bare CF, (f) SEM image of cobalt hydroxide nanoflakes coated on CF (Inset: magnified SEM image of the nanoflakes), (g) variation of specific capacitance with mass loading of each electrode, (h) specific capacitances of CF electrode at scan rates of 5, 10, 20, 50 and 100 mV/s, (i) schematic of flexible SC fabrication, (j) CV curves at bending conditions of 0° and 180° at scan rate of 20 mV/s [56].

and deposited an ultrathin nickel hydroxide film on carbon-coated 3D porous copper structure in order to prepare binder-free conductive electrode (**Figure 5(a-b)**) [53]. This electrode has short electron path distances and large electrochemical active sites, which improved structural stability for high performance SCs. A carbon coating was used to improve the electron transport behavior and to prevent the oxidation of Cu. Nickel hydroxide supported on mesoporous hollow dendritic three-dimensional-nickel exhibited a specific capacitance of 1860 F g^{-1} at a current density of 1 A g^{-1} (**Figure 5(c)**). It could retain 86.5% capacitance over 10,000 cycles. Tang *et al.* have prepared an additive-free, nano-architectured nickel hydroxide/carbon nanotube (Ni(OH)₂/CNT) electrode for high performance SCs [54]. This Ni(OH)₂/CNT electrode was fabricated by depositing Ni(OH)₂ nano-flakes on CNT bundles which were directly grown on Ni foams. The above electrode exhibited the specific capacitance of 3300 F g^{-1} and an aerial capacitance of 16 Fcm^{-2}. Ma *et al.* have synthesized electrode of Ni(OH)₂ nanosheet/3D GF framework using two methods, CVD and hydrothermal [55]. They have compared the capacitive properties of Ni(OH)2 electrode/graphene fiber with Ni(OH)₂/Ni foam and Ni(OH)₂ nanosheet/carbon fiber cloth electrodes. Ni(OH)₂ electrode with graphene fiber exhibited better performance in terms of specific capacitance and rate capability. The Ni(OH)₂ nanosheet/graphene fiber electrode exhibited electrochemical capacitance as high as 2860 F g^{-1} at a current density of 2 A g^{-1}, and maintains 1791 F g^{-1} at 30 A g^{-1}.

5.2 Carbon-cobalt hydroxide (Co(OH)₂) composite electrode materials

Co(OH)₂ has recently received increasing attention as electrode for SC application because of its low cost and high capacitance. Jagadale *et al.* have used cobalt hydroxide nanoflakes which were uniformly loaded on flexible carbon fiber (CF)

paper as electrode for SC (**Figure 5(d)**) [56]. The carbon fiber was basically used to provide unique porous nanostructure offering low ion diffusion and charge transfer resistance to the electrode (**Figure 5(e, f)**). The electrode exhibited maximum specific capacitance of 386.5 F g^{-1} at a current density of 1 mA cm^{-2} with a mass loading of 2.5 mg cm^{-2} (**Figure 5(g, h)**). An energy density of 133.5 W h kg^{-1} has been obtained with power density of and 1769 W kg^{-1}. The carbon fiber has improved the cyclic stability of 92% over 2000 cycles. To check applicability of electrodes, these electrodes further employed to fabricate flexible solid state supercapacitor. CV curves of SC at bending conditions of 0° and 180° at scan rate of 20 mV/s. It is clearly seen that the area under curve doesn't change significantly after bending which proves that SC is highly flexible and does not lose its structural integrity under bending conditions (**Figure 5(i, j)**).

Two possible reactions are suggested for the electrochemical reactions of Co(OH)$_2$ in KOH electrolyte [57]:

$$Co(OH)_2 + OH^- = CoOOH + H_2O + e^- \qquad (6)$$

$$CoOOH + OH^- = CoO_2 + H_2O + e^- \qquad (7)$$
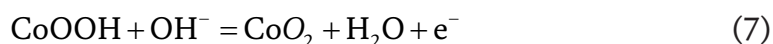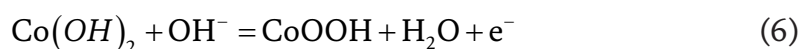
Co(OH)$_2$ nano-sheet-decorated graphene-CNT composite structure has been designed for SC application [58]. Suspensions method was used to prepare graphene-CNT composite by sonication and vacuum filtration. The graphene-CNT composite may offer high porosity with high conductivity, chemical stability and a three-dimensional structure. The vertically aligned Co(OH)$_2$ nano-sheets were then deposited on 3D graphene-CNT composite by solution based process. The ASC of Co(OH)$_2$ with graphene-CNT has shown a specific capacitance of 310 F g^{-1}. The electrode exhibited an energy density of 172 W h kg^{-1} and maximum power density of 198 kW kg^{-1} in ionic liquid electrolyte 1-ethyl-3-methylimidazoliumbis (trifluoromethanesulfone)imide (EMI-TFSI). Zhang *et al.* have deposited Co(OH)$_2$ on multi-walled CNT which were grown on the carbon paper substrate [59]. The composite electrode showed the specific capacitance of 1083 F g^{-1} determined at a current density of 0.83 A g^{-1} in aqueous electrolyte. CNTs were added to Co(OH)$_2$ in order to improve the electrical conductivity of the electrode. The interconnected nanosheets of the Co(OH)$_2$ would help to facilitate the contact of the electrolyte with active materials, exhibiting good cycling stability and lifetime.

5.3 Carbon-iron oxy hydroxide (FeOOH) composite electrode materials

FeOOH has been recognized is an attractive electrode material for SC due to low cost, high theoretical specific capacitance, and broad potential window. In addition, the unique tunnel structure of FeOOH with open permeable channels are beneficial for ion transportation and shorten the diffusion path for electrolyte ion diffusion [60]. However, the poor electrical conductivity and low specific surface area limited the use of FeOOH as a potential electrode for SC, which limited specific capacitance and rate capability [61]. Alternatively, composite system by assembling FeOOH on the carbon based supporting materials (AC, carbon black, graphene, etc.) can be enhance the capacitive performance. Shen *et al.* synthesized radiating γ-FeOOH Nanosheets on CC substrate (γ-FeOOH NSs/CC) by a simple one-step electrodeposition method and investigated its pseudocapacitive behaviour in a typical ionic liquid [1-ethyl-3-methylimidazolium bis imide (EMIM-NTF2)] through electrochemical quartz crystal microbalance (EQCM). The charge storage is mainly due
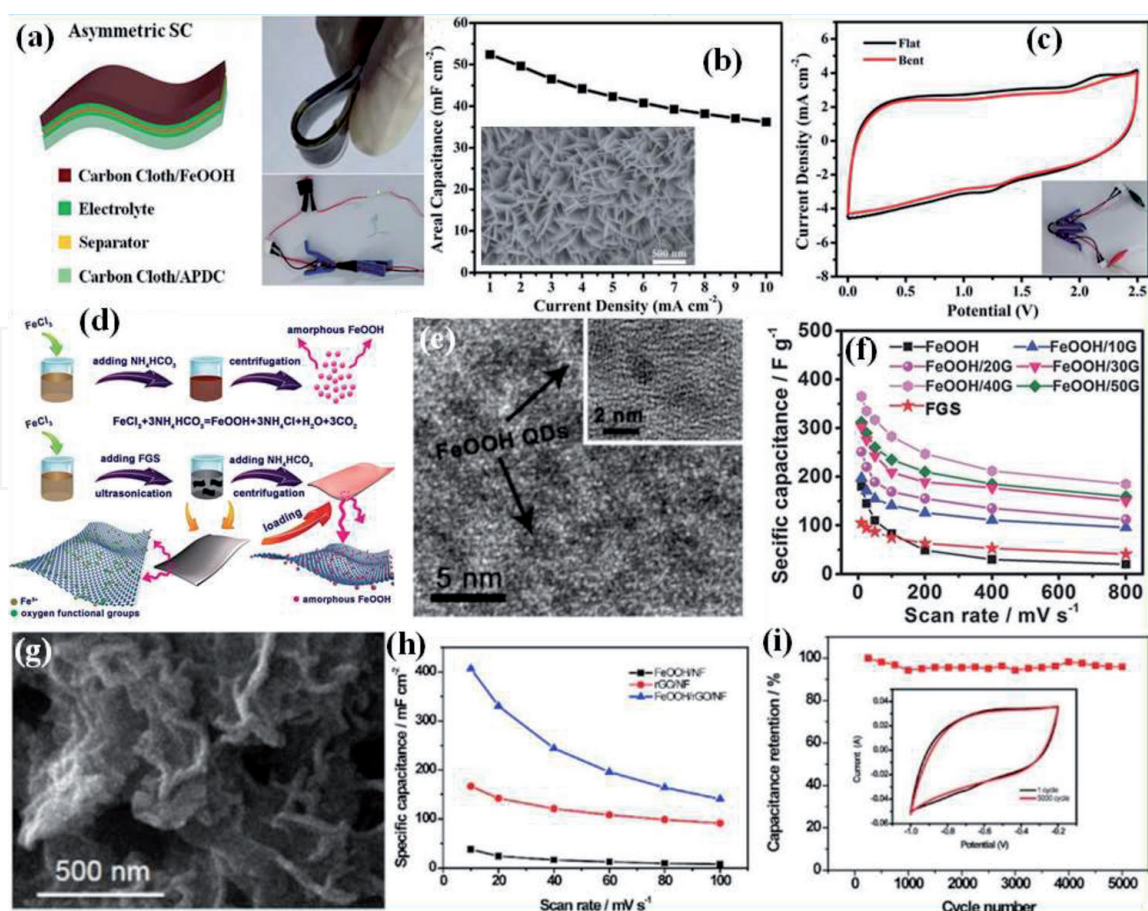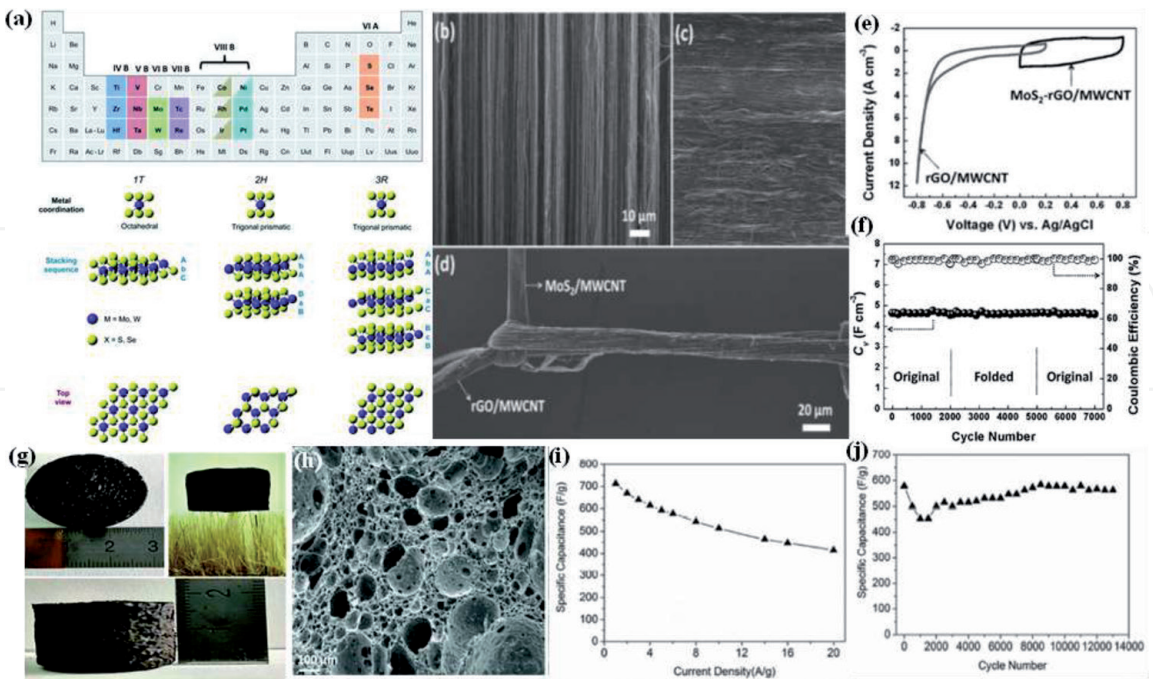
Figure 6.
(a) Schematic illustrations of the fabrication procedure for the FeOOH//APDC f-SSC electrodes and flexibility and operating status as supercapacitor device, (b) The areal capacitance as a function of the discharge current density (Inset: SEM images of as-prepared γ-FeOOH nanosheets on a carbon cloth substrate), (c) CV curves of the FeOOH//APDC f-SSC at bent and flat statuses [62]. (d) Schematic illustration of the synthesis of amorphous FeOOH QDs and amorphous FeOOH/FGS hybrid nanosheets, (e) HRTEM images of the FeOOH QDs (Inset: enlarged HRTEM for FeOOH QDs), (f) The specific capacitances of the FeOOH, functionalized graphene sheet (FGS), and FeOOH/FGS composite electrodes as a function of the scan rate [64]. (g) High-magnification SEM images of as-prepared 3D FeOOH/rGO/NF, (h) Areal capacitance of FeOOH/NF, rGO/ NF and FeOOH/rGO/NF electrodes calculated from CV curves as a function of scan rate, and (i) Cycling performance of MnO₂//FeOOH-ASC collected at a scan rate of 100 mV s⁻¹ for 5000 cycles [66].

to the insertion and extraction of [EMIM]$^+$ cations through the transport pathways offered by the crystalline network of γ-FeOOH during charging-discharging process. γ-FeOOH NSs/CC exhibited a good areal capacitance of 210 mF cm^{-2} at a current density of 1 mA cm^{-2} and the ASC device made of γ-FeOOH‖APDC (activated polyaniline-derived carbon nanorods) solid-state flexible SCs acquired a high energy density of 1.44 mW h cm^{-3} at a current density of 3 A g^{-1} with a cycling stability of 80.5% retention over 2000 cycles (**Figure 6(a-c)**) [62]. An amorphous FeOOH nanoflowers@multi-walled CNT (FeOOH NFs@ MWCNTs) composite was prepared by Sun *et al.* [63]. The as-prepared composite electrode displays a high specific capacitance of 345 F g^{-1} at 1 A g^{-1} current density and outstanding rate performance (167 F g^{-1} at 11.4 A g^{-1}) with good cycling stability of 76.4% over 5000 cycles. The outstanding electrochemical performance of the composite electrode is due to the mesoporous structure and high surface area of the electrode materials as well as fast ion/electronic transport and easy accessibility of the active materials to electrolytes. Liu *et al.* demonstrated FeOOH quantum dots (QDs)/graphene hybrid nanosheets, which exhibited a high specific capacitance of 365 F g^{-1} at a current density of 1 A g^{-1} with excellent capacitance retention of 89.7% of initial capacitance over 20000 cycles as well as a great rate capability (189 F g^{-1} at a high current density of 128 A g^{-1}) (**Figure 6(d-f)**) [64]. In addition, specific capacitance

of the SC increased to 1243 F g^{-1} at 5 mV s^{-1} while the voltage window was extended from -0.8 to 0 V to -1.25 to 0 V but the cycling performance declined sharply. Wei *et al.* synthesized ultrathin α-FeOOH nanorods/graphene oxide (GO) composite by hydrothermal method, which exhibited high specific capacitance of 127 F g^{-1} at a current density of 10 A g^{-1}, good cyclic performance of 85% capacitance retention over 2000 cycles, and excellent rate capability (100 F g^{-1} at 20 A g^{-1}) as compared to than bare α-FeOOH nanorods [65]. The outstanding electrochemical performance of α-FeOOH nanorods/GO composite is due to its unique structure, which provides fast electron/ions transport and high charging/discharging rate. 3D FeOOH/reduced graphene oxide/Ni foam (FeOOH/rGO/NF) based hybrid electrodes fabricated by the electrodeposition of FeOOH nanosheets on the rGO/Ni foam surface exhibited an exception high areal capacitance of 406.5 mF cm^{-2} at a scan rate of 10 mV s^{-1}, which is 10-fold higher than the bare FeOOH/NF electrode (**Figure 6(g-i)**) [66]. This high areal capacitance of FeOOH/rGO/NF is due to the improved conductivity and increased surface area, which not only provide a superior pathway for electron transfer, but also offer more active sites for energy storage. In addition, an ASC device made of 3D FeOOH/rGO/NF electrode as anode and MnO$_2$@TiN electrode as cathode attained a remarkable maximum power density of 0.19 W cm^{-3} with maximum energy density of 0.48 mW h cm^{-3}.

6. Carbon-transition metal dichalcogenides (TMDs) composite electrode materials

TMDs are layered inorganic materials with a chemical configuration of MX$_2$, in which M is a transition metal element (M: Ti, Mo, V, W, Re, Ta), and X can be any chalcogenide element (X: S, Se, Te) (**Figure 7(a)**). Each MX$_2$ unit cell is stacked

Figure 7.
(a) Different metal coordination and stacking sequence in TMD unit cells [67]. (b-d) SEM images of aligned MWCNT sheets, MWCNT/MoS$_2$ hybrids, and tightly knotted MoS$_2$/MWCNT and rGO/MWCNT fibers, respectively. (e) CV curves of rGO/MWCNT (cathode) and MoS$_2$-rGO/MWCNT (anode) at different potential windows. (f) Cycle stability test of the fiber-based asymmetric device at 0.55 A cm^{-3} current density [74]. (g) Optical photographs and (h) SEM images of the MoS$_2$/C composite aerogel. (i) specific capacitances at different current densities and (j) long-term cycle stability at a current density of 6 A g^{-1} of the MoS$_2$/C composite aerogel electrode material [75].

together through Vander Waals force in such a way that transition metal layer is present in between the two chalcogen sheets [67]. On the basis of crystal structure, there are two types of phases of TMDs, which are metallic 1T phase with an octahedral structure and semiconducting 2H phase with a trigonal structure. Recently, TMDs have been attracted great attention as SC electrode materials due to their large surface area, low cost, variable oxidation states, high mechanical properties, high chemical stability and easy synthesis [68]. The variable oxidation states, large surface area, and active edges of TMDs allow electrical double layer and fast/reversible redox charge storage mechanisms and offer high energy storage capability in SCs. However, due to the inherently low conductivity, poor cycle life, large volume change during cycling and restacking limits their electrochemical performance as SC electrodes [69]. For example, Soon *et al.* has synthesized sheet-like morphology of MoS_2 by chemical vapor deposition method, which has a very large surface area favorable for double layer storage. But due to its poor electrical conductivity, it showed low specific capacitance of ~100 F g^{-1} at a scan rate of 1 mV s^{-1} [70]. Therefore, in order to improve the electrochemical performance of TMDs, they have been compositing with highly conducting/electroactive carbon based supporting materials by various top-down/bottom-up and both synthetic approaches. The synergic effect of carbon-TMDs based composite materials such as carbon offers conductive channels and increasing the interfacial contact, whereas TMDs provide a short ion diffusion path and followed by short electron transport path enhances the overall electrochemical performance of the SC.

6.1 Carbon-MoS_2 composite electrode materials

MoS_2/MWCNT nanocomposite synthesized by a hydrothermal method exhibited a large surface area and fast ionic transport properties and showed a high specific capacitance of 452.7 F g^{-1} with good cycling stability (95.8% retention after 1000 cycles), which is almost three times larger than the bare MoS_2 (149.6 to 452.7 F g^{-1}) [71]. Ali *et al.* fabricated MoS_2/graphene composite from bulk MoS_2 and graphite rod through facile electrochemical exfoliation method and exhibited high specific capacitance of 227 F g^{-1} as compared with the exfoliated MoS_2 (70 F g^{-1}) and exfoliated graphene (85 F g^{-1}) at a current density of 0.1 A g^{-1} [72]. The high specific capacitance of MoS_2/graphene composite is due to the synergistic effect between MoS_2 and graphene. Ali *et al.* demonstrated the electrochemical performance of MoS_2/CNT/GNF composite and compared the performance with MoS_2/CNTs, MoS_2/graphene nanoflakes [73]. It has been noticed that the electrochemical charge storage performance has been improved by incorporation of the carbon materials into the composite and the composite showed a maximum specific capacitance of 104 F g^{-1} at a current density of 0.5 A g^{-1} with capacitance retention of 75% after the 1000 cycle at a scan rate of 10 mV/s. Another interesting MoS_2-rGO/MWCNT fiber electrode was fabricated by incorporating rGO nanosheets and MoS_2 into aligned MWCNT, which operated at a stable potential window of 1.4 V and exhibited high coulombic efficiency of 100% over 7000 cycles in the bending state (**Figure 7(b-f)**) [74]. Zhang *et al.* reported an agarose induced technique to synthesize MoS_2/carbon composite aerogel, which showed a high specific capacitance of 712.6 F g^{-1} at a current density of 1 A g^{-1} with cyclic stability of 97.3% over 13000 charge-discharge cycles (**Figure 7(g-j)**) [75]. The high specific capacitance of MoS_2/carbon composite aerogel is because of 3D intercalated network with hierarchal porous and interlayer MoS_2 expanded structures, which were beneficial for easy ion transportation. 3D graphene/MoS_2 composite electrode material has been synthesized by Sun et al and co-workers through a simple and facile one-step hydrothermal process [76]. The as-synthesized composite electrode exhibited

gravimetric capacitance of 410 F g^{-1} at a current density of 1 A g^{-1} and an excellent cycling stability of 80.3% over 10,000 continuous charge-discharge cycles at 2 A g^{-1} current density. The outstanding electrochemical performance of 3D graphene/ MoS$_2$ composite electrode is due to the 3D architecture of conducting network graphene and flower-like structure of MoS$_2$, which enhances the electrolyte ions diffusion process.

6.2 Carbon-WS$_2$ composite electrode materials

WS$_2$ nanoplates supported on carbon fiber cloth (WS$_2$/CFC) have been synthesized by a facile solvothermal process and used as electrode material for SC [77]. The 3D network of CFC not only prevent the agglomeration of WS$_2$ nano-plates but also enhances the ion transport efficiency due to low charge transfer resistance (R$_{ct}$) of 0.1 Ω. The as fabricated WS$_2$/CFC electrode exhibited a high specific capacitance of 399 F g^{-1} at 1 A g^{-1} current density with cyclic retention of 99% over charge-discharge 500 cycles, which is higher than compared with bare WS$_2$. In addition, developing such composite of WS$_2$ with the carbon fibre helps for fabricating wearable SCs which are in demand for wearable electronics. Yang *et al.* fabricated WS$_2$@CNT hybrid film electrode by incorporating conducting CNTs into WS$_2$. The WS$_2$@CNT hybrid film with a unique skeleton structure showed a maximum specific area capacitance of 752.53 mF cm^{-2} at a scan rate 20 mV s^{-1} with very good cyclic stability by only loss of 1.28% capacitance after 10,000 cycles. In addition, a quasi-solid-state flexible SC made by WS$_2$@CNT hybrid film exhibited excellent bendability under bending to 135 10, 000 times with the loss of 23.12% at scan rate of 100 mV s^{-1} [53]. Tu *et al.* have been synthesized WS$_2$/RGO hybrid material by using a simple molten salt process, which showed a high specific capacitance of 2508.07 F g^{-1} at 1 mV s^{-1} scan rate with excellent capacitance retention of 98.6% over 5000 cycles, due to synergic effect of highly conducting RGO and large charge-accumulating sites of WS$_2$ networks. Likewise, Xu *et al.* demonstrated 3D composite of WS$_2$ nanoflakes and quantum dots on N and S co-doped reduced graphene oxide (WS$_2$/N,S-rGO) crumpled nanosheets through a rapid solution combustion synthesis of the precursor and subsequent gas-solid phase sulfurization process, which presented a significant specific capacitance of 1562.5 F g^{-1} at 1 A g^{-1} current density, and a rate capabil-ity of 780 F g^{-1} at 40 A g^{-1} (**Figure 8(a-c)**) [78]. The high specific capacitance of WS$_2$/N,S-rGO hybrids is because of synergistic effect between WS$_2$ and N,S-rGO, where N,S-rGO provides larger contact surface area, excellent charge transport, and shorter ion diffusion path. Hierarchical MoSe$_2$/C hybrid was successfully fab-ricated by facile one-step hydrothermal strategy, which composed of few-layered MoSe$_2$ nanosheets and amorphous carbon obtained from the decomposition of the triethylene glycol. As fabricated hierarchical MoSe$_2$/C electrode exhibited high specific capacitance of 878.6 F g^{-1} in comparison with the bare MoSe$_2$ at current density of 1 A g^{-1} and maintained 98% of initial capacitance over 2000 cycles without obvious decrease. The superior electrochemical performances of MoSe$_2$/C hybrid can be ascribed to hierarchical structure of MoSe$_2$ and conducting nature of carbon, which help for providing large surface area for electrochemical reac-tions and enhancing charge carriers transfer at the electrolyte/electrode interface [79]. Liu *et al.* fabricated VACNTF@MoSe$_2$/NF composite electrode through a combined chemical vapor deposition method and solvothermal methods by growing MoSe$_2$ nanoflakes on the vertically aligned carbon nanotube array film (VACNTF) with binder-free nickel foam as current collector [80]. The as fabri-cated VACNTF@MoSe$_2$/NF composite electrode exhibited high specific capaci-tance of 435 F g^{-1} at a current density of 1 A g^{-1} with outstanding cycling stability
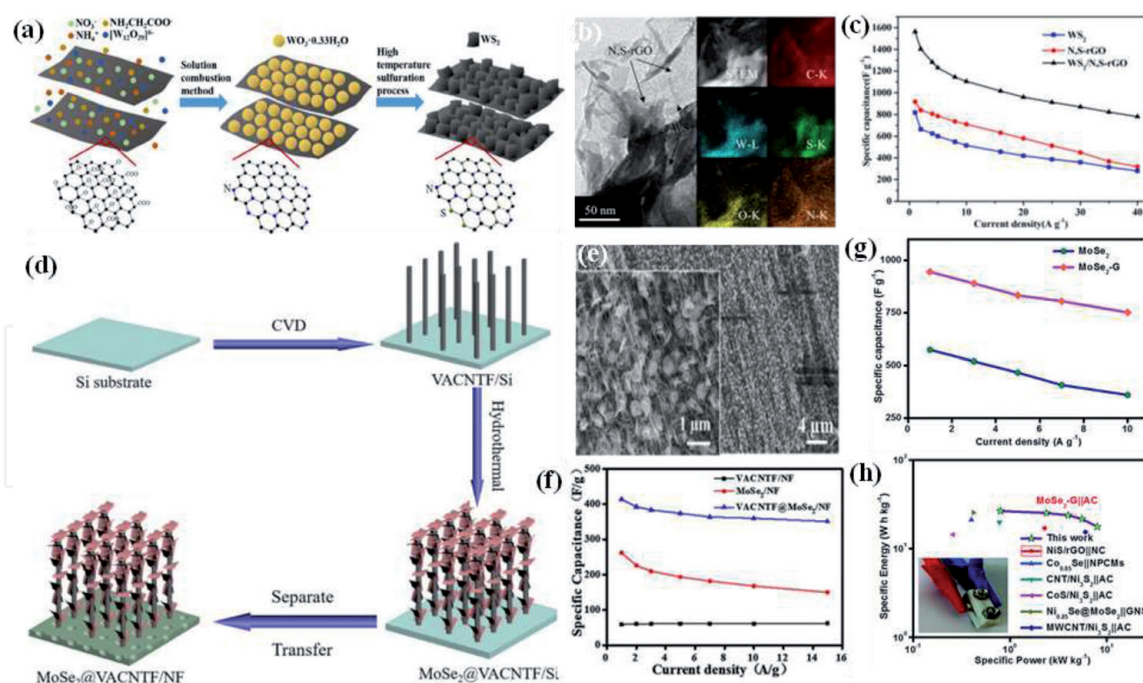
Figure 8.
(a) Schematic illustration of synthetic processes of WS$_2$/N,S-rGO hybrid, (b) HRTEM, STEM and EDS elemental mapping images of WS$_2$/N,S-rGO hybrid, and (c) The specific capacitances of the WS$_2$, N,S-rGO and WS$_2$/N,S-rGO hybrid at different current densities [78]. (d) Schematic illustration of the synthesis process of the VACNTF@MoSe$_2$/NF composite electrode, (e) SEM images of the VACNTF@MoSe$_2$ composites (inset: high magnification), and (f) The specific capacitance comparison of the MoSe$_2$/NF, VACNTF/NF and VACNTF@MoSe$_2$/NF electrodes at various current densities [80]. (g) Specific capacitance of the MoSe$_2$ NS and MoSe$_2$/G nanohybrid based electrodes as a function of current density, and (h) Ragone plot for the MoSe$_2$G||AC ASC device (inset: photograph of ASC device) [81].

of 92% after 5000 cycles (**Figure 8(d-f)**). In addition, the VACNTF@MoSe$_2$/NF composite based ASC displays a high energy density with 22 W h kg^{-1} for a power density of 330 W kg^{-1}. Kirubasankar *et al.* MoSe$_2$/graphene nanohybrid based electrode prepared by a simple and facile sonochemical route, which showed higher specific capacitance (945 F g^{-1}) as compared to MoSe$_2$ nanosheets (576 F g^{-1}) at 1 A g^{-1} current density. Further, as fabricated ASC device based on MoSe$_2$/graphene nanohybrid retains 88% of its capacitance over 3000 cycles and delivers an energy density of 26.6 W h kg^{-1} at a power density of 0.8 kW kg^{-1} (**Figure 8(g, h)**) [81]. The high specific capacitance with better rate capability is due to the effective penetration and migration of electrolyte, reduction of the contact resistance and shortness of the diffusion path of ions between the electrode-electrolyte interface, which enhances the redox kinetics and provide maximum utilization of the electroactive area, so providing a high structural stability during charge-discharge processes. Similarly, Huang *et al.* demonstrated MoSe$_2$/graphene on flexible Ni electrode, which could deliver a specific capacitance of 1422 F g^{-1} and fully retention of initial capacitance over 1500 cycles [82]. Wei *et al.* first time fabricated free-standing SC anode based on 3D MoSe$_2$ nanoflowers (MoSe$_2$ NFs) and hierarchically porous anisotropic carbonized delignified wood (CDW), which exhibited ultrahigh capacitance of 1043 mF cm^{-2} at a current density of 1 mA cm^{-2} and excellent cycling stability less than 5% capacitance loss over 5000 cycles. The ASC device was made by integration of 3D MoSe$_2$ NFs@CDW anode and a common MnO$_2$-based cathode, which exhibited a high capacitance of 415 mF cm^{-2} at a current density of 2.5 mA cm^{-2} with high energy density of 147 mW h cm^{-2} at power density of 2 mW cm^{-2}. These results confirm that 3D MoSe$_2$ NFs@CDW based anode can be used as a potential anode for the development of high-performance SCs [83].

7. Conclusion

In the past few decades, SCs have been extensively studied as energy storage devices and more focusing area in the multidisciplinary science over the world. The selection of high performance SC electrode materials based on high specific capacitance, low internal resistance and good stability. In this article, we have reviewed the carbon-based composite materials (*i.e.*, metal oxide, metal hydroxide, TMDs composited with carbon materials) as promising SC electrode materials due to the synergic effect of the composite materials such as high surface area, interconnected porous structure, high electrical conductivity, excellent wettability towards the electrolyte, and presence of electrochemically active surface functionalities of the carbon supports which improves the EDL capacitance while metal oxide or metal hydroxide or TMDs enhances electrochemical performance through pseudocapacitive/faradaic charge-storage process. The carbon-based composite materials demonstrated herein usually possesses high specific capacity, impressive energy density and maintain long term stability with better mechanical flexibility. We also observe the microstructural changes in the carbon-based composite materials would be more favorable for fabrication of high performance supercapacitor. We also explained how the composite materials overcome the traditional obstacles while formulating the standard electrode designs as compare to individual components.

Acknowledgements

Author details

Prasanta Kumar Sahoo[1], Chi-Ang Tseng[2], Yi-June Huang[3] and Chuan-Pei Lee[4*]

1 Department of Mechanical Engineering, Siksha 'O' Anusandhan, Deemed to be University, Bhubaneswar, Odisha, India

2 Department of Chemistry, National Taiwan University, Taipei, Taiwan

3 Graduate Institute of Nanomedicine and Medical Engineering, College of Biomedical Engineering, Taipei Medical University, Taipei, Taiwan

4 Department of Applied Physics and Chemistry, University of Taipei, Taiwan

*Address all correspondence to: CPLee@utaipei.edu.tw

IntechOpen

References

[1] Yu Z., Duong B., Abbitt D., Thomas J., Highly ordered MnO_2 nanopillars for enhanced supercapacitor performance. Adv Mater. 2013; 25; 3302-3306, DOI: 10.1002/adma.201300572.

[2] Etacheri Vinodkumar, Marom Rotem, Elazari Ran, Salitra Gregory, Aurbach Doron, Challenges in the development of advanced Li-ion batteries: a review. Energy & Environmental Science. 2011; 4; 3243, DOI: 10.1039/c1ee01598b.

[3] Miller John R., Simon Patrice, Electrochemical Capacitors for Energy Management. Science. 2008; 321; 651-652, DOI: DOI: 10.1126/science.1158736.

[4] Naoi Katsuhiko, Nao Wako, Aoyagi Shintaro, Miyamoto Jun-ichi, Kamino Takeo, New Generation "Nanohybrid Supercapacitor". Accounts of Chemical Research. 2013; 46; 1075-1083, DOI: https://doi.org/10.1021/ar200308h.

[5] Choudhary N., Li C., Moore J., Nagaiah N., Zhai L., Jung Y., Thomas J., Asymmetric Supercapacitor Electrodes and Devices. Adv Mater. 2017; 29, DOI: 10.1002/adma.201605336.

[6] Meng C., Gall O. Z., Irazoqui P. P., A flexible super-capacitive solid-state power supply for miniature implantable medical devices. Biomed Microdevices. 2013; 15; 973-983, DOI: 10.1007/s10544-013-9789-1.

[7] Zhang Li Li, Zhou Rui, Zhao X. S., Graphene-based materials as supercapacitor electrodes. Journal of Materials Chemistry. 2010; 20; 5983, DOI: 10.1039/c000417k.

[8] Ke Qingqing, Wang John, Graphene-based materials for supercapacitor electrodes – A review. Journal of Materiomics. 2016; 2; 37-54, DOI: 10.1016/j.jmat.2016.01.001.

[9] Wang G., Zhang L., Zhang J., A review of electrode materials for electrochemical supercapacitors. Chem Soc Rev. 2012; 41; 797-828, DOI: 10.1039/c1cs15060j.

[10] Zou Yong, Han Bu-Xing, High-Surface-Area Activated Carbon from Chinese Coal. Energy & Fuels. 2001; 15; 1383-1386, DOI: https://doi.org/10.1021/ef0002851.

[11] Zhu Y., Murali S., Cai W., Li X., Suk J. W., Potts J. R., Ruoff R. S., Graphene and graphene oxide: synthesis, properties, and applications. Adv Mater. 2010; 22; 3906-3924, DOI: 10.1002/adma.201001068.

[12] Portet C., Yushin G., Gogotsi Y., Electrochemical performance of carbon onions, nanodiamonds, carbon black and multiwalled nanotubes in electrical double layer capacitors. Carbon. 2007; 45; 2511-2518, DOI: 10.1016/j.carbon.2007.08.024.

[13] Lota Grzegorz, Fic Krzysztof, Frackowiak Elzbieta, Carbon nanotubes and their composites in electrochemical applications. Energy & Environmental Science. 2011; 4; 1592, DOI: 10.1039/c0ee00470g.

[14] Geim A. K., Novoselov K. S., The rise of graphene. Nature Materials. 2007; 6; 183-191, DOI: https://doi.org/10.1038/nmat1849.

[15] Simon PATRICE, Gogotsi Yury, Materials for electrochemical capacitors. Nature Materials. 2008; 7; 845-854, DOI: https://doi.org/10.1038/nmat2297.

[16] Simon P., Gogotsi Y., Capacitive Energy Storage in Nanostructured Carbon-Electrolyte Systems. Accounts of Chemical Research. 2013 46; 1094-1103, DOI: https://doi.org/10.1021/ar200306b.

[17] Trasatti Sergio, Buzzanca Giovanni, Ruthenium dioxide: A new interesting electrode material. Solid state structure and electrochemical behaviour. Journal of Electroanalytical Chemistry and Interfacial Electrochemistry. 1971 29; A1-A5, DOI: https://doi.org/10.1016/S0022-0728(71)80111-0.

[18] Lee Hee Y., Goodenough J. B., Supercapacitor Behavior with KCl Electrolyte. Journal of Solid State Chemistry. 1999; 144; 220-223, DOI: https://doi.org/10.1006/jssc.1998.8128.

[19] Wu Nae-Lih, Nanocrystalline oxide supercapacitors. Materials Chemistry and Physics. 2002 75; 6-11, DOI: https://doi.org/10.1016/S0254-0584(02)00022-6.

[20] Reddy A. Leela Mohana, Ramaprabhu S., Nanocrystalline Metal Oxides Dispersed Multiwalled Carbon Nanotubes as Supercapacitor Electrodes. The Journal of Physical Chemistry C. 2007; 111; 7727-7734, DOI: https://doi.org/10.1021/jp069006m.

[21] Ho M. Y., Khiew P. S., Isa D., Tan T. K., Chiu W. S., Chia C. H., A Review of Metal Oxide Composite Electrode Materials for Electrochemical Capacitors. Nano. 2014; 09; 1430002, DOI: 10.1142/s1793292014300023.

[22] Chen Yan-Li, Hu Zhong-Ai, Chang Yan-Qin, Wang Huan-Wen, Zhang Zi-Yu, Yang Yu-Ying, Wu Hong-Ying, Zinc Oxide/Reduced Graphene Oxide Composites and Electrochemical Capacitance Enhanced by Homogeneous Incorporation of Reduced Graphene Oxide Sheets in Zinc Oxide Matrix. The Journal of Physical Chemistry C. 2011; 115; 2563-2571, DOI: 10.1021/jp109597n.

[23] Rolison D. R., Long J. W., Lytle J. C., Fischer A. E., Rhodes C. P., McEvoy T. M., Bourg M. E., Lubers A. M., Multifunctional 3D nanoarchitectures for energy storage and conversion. Chem Soc Rev. 2009; 38; 226-252, DOI: 10.1039/b801151f.

[24] Wu Z., Li L., Yan J. M., Zhang X. B., Materials Design and System Construction for Conventional and New-Concept Supercapacitors. Adv Sci (Weinh). 2017; 4; 1600382, DOI: 10.1002/advs.201600382.

[25] Fischer Anne E., Pettigrew Katherine A., Rolison Debra R., Stroud Rhonda M., Long Jeffrey W., Incorporation of Homogeneous, Nanoscale MnO_2 within Ultraporous Carbon Structures via Self-Limiting Electroless Deposition: Implications for Electrochemical Capacitors. Nano Letters. 2007; 7; 281-286, DOI: https://doi.org/10.1021/nl062263i.

[26] Hwang Jee Y., El-Kady Maher F., Wang Yue, Wang Lisa, Shao Yuanlong, Marsh Kristofer, Ko Jang M., Kaner Richard B., Direct preparation and processing of graphene/RuO_2 nanocomposite electrodes for high-performance capacitive energy storage. Nano Energy. 2015; 18; 57-70, DOI: 10.1016/j.nanoen.2015.09.009.

[27] Suktha Phansiri, Phattharasupakun Nutthaphon, Sawangphruk Montree, Transparent supercapacitors of 2 nm ruthenium oxide nanoparticles decorated on a 3D nitrogen-doped graphene aerogel. Sustainable Energy & Fuels. 2018; 2; 1799-1805, DOI: 10.1039/c8se00177d.

[28] Zhang K., Han X., Hu Z., Zhang X., Tao Z., Chen J., Nanostructured Mn-based oxides for electrochemical energy storage and conversion. Chem Soc Rev. 2015; 44; 699-728, DOI: 10.1039/c4cs00218k.

[29] Wei W., Cui X., Chen W., Ivey D. G., Manganese oxide-based materials as electrochemical supercapacitor electrodes. Chem Soc Rev. 2011; 40; 1697-1721, DOI: 10.1039/c0cs00127a.

[30] Gao Peng-Cheng, Lu An-Hui, Li Wen-Cui, Dual functions of activated carbon in a positive electrode for MnO$_2$-based hybrid supercapacitor. Journal of Power Sources. 2011; 196; 4095-4101, DOI: 10.1016/j.jpowsour.2010.12.056.

[31] Huang Huajie, Zhang Wenyao, Fu Yongsheng, Wang Xin, Controlled growth of nanostructured MnO$_2$ on carbon nanotubes for high-performance electrochemical capacitors. Electrochimica Acta. 2015; 152; 480-488, DOI: 10.1016/j.electacta.2014.11.162.

[32] Yan Jun, Fan Zhuangjun, Wei Tong, Qian Weizhong, Zhang Milin, Wei Fei, Fast and reversible surface redox reaction of graphene–MnO$_2$ composites as supercapacitor electrodes. Carbon. 2010; 48; 3825-3833, DOI: 10.1016/j.carbon.2010.06.047.

[33] Zhang Zheye, Xiao Fei, Wang Shuai, Hierarchically structured MnO$_2$/graphene/carbon fiber and porous graphene hydrogel wrapped copper wire for fiber-based flexible all-solid-state asymmetric supercapacitors. Journal of Materials Chemistry A. 2015; 3; 11215-11223, DOI: 10.1039/c5ta02331a.

[34] Fang Cuiqin, Zhang Dong, A large areal capacitance structural supercapacitor with a 3D rGO@MnO$_2$ foam electrode and polyacrylic acid–Portland cement–KOH electrolyte. Journal of Materials Chemistry A. 2020; 8; 12586-12593, DOI: 10.1039/d0ta03109g.

[35] He Guangyu, Li Jianghua, Chen Haiqun, Shi Jian, Sun Xiaoqiang, Chen Sheng, Wang Xin, Hydrothermal preparation of Co$_3$O$_4$@graphene nanocomposite for supercapacitor with enhanced capacitive performance. Materials Letters. 2012; 82; 61-63, DOI: 10.1016/j.matlet.2012.05.048.

[36] Xia Xin-hui, Tu Jiang-ping, Zhang Yong-qi, Mai Yong-jin, Wang Xiu-li, Gu Chang-dong, Zhao Xin-bing, Freestanding Co$_3$O$_4$ nanowire array for high performance supercapacitors. RSC Advances. 2012; 2; 1835, DOI: 10.1039/c1ra00771h.

[37] Iqbal Muhammad Zahir, Haider Syed Shabhi, Zakar Sana, Alzaid Meshal, Afzal Amir Muhammad, Aftab Sikandar, Cobalt-oxide/carbon composites for asymmetric solid-state supercapacitors. Materials Research Bulletin. 2020; 131; 110974, DOI: 10.1016/j.materresbull.2020.110974.

[38] Sun Juan, Man Ping, Zhang Qichong, He Bing, Zhou Zhenyu, Li Chaowei, Wang Xiaona, Guo Jiabin, Zhao Jingxin, Xie Liyan, Li Qingwen, Sun Jing, Hong Guo, Yao Yagang, Hierarchically-structured Co$_3$O$_4$ nanowire arrays grown on carbon nanotube fibers as novel cathodes for high-performance wearable fiber-shaped asymmetric supercapacitors. Applied Surface Science. 2018; 447; 795-801, DOI: 10.1016/j.apsusc.2018.03.244.

[39] Tan Hui Yun, Yu Bao Zhi, Cao Lin Li, Cheng Tao, Zheng Xin Liang, Li Xing Hua, Li Wei Long, Ren Zhao Yu, Layer-dependent growth of two-dimensional Co$_3$O$_4$ nanostructure arrays on graphene for high performance supercapacitors. Journal of Alloys and Compounds. 2017; 696; 1180-1188, DOI: 10.1016/j.jallcom.2016.12.050.

[40] Tseng C. A., Sahoo P. K., Lee C. P., Lin Y. T., Xu J. H., Chen Y. T., Synthesis of CoO-Decorated Graphene Hollow Nanoballs for High-Performance Flexible Supercapacitors. ACS Appl Mater Interfaces. 2020; 12; 40426-40432, DOI: 10.1021/acsami.0c12898.

[41] Zomorodian Esfahani Majid, Aghaei Alireza, Khosravi Mohsen, Bagheri Narjes, Khakpour Zahra, Javaheri Masoumeh, Pore structure improvement of carbon aerogel and investigation of the supercapacitive behavior of a Co$_3$O$_4$ nanoball/carbon

aerogel composite. New Journal of Chemistry. 2017; 41; 11731-11741, DOI: 10.1039/c7nj02897k.

[42] Zhu Yun Guang, Wang Ye, Shi Yumeng, Huang Zhi Xiang, Fu Lin, Yang Hui Ying, Phase Transformation Induced Capacitance Activation for 3D Graphene-CoO Nanorod Pseudocapacitor. Advanced Energy Materials. 2014; 4; 1301788, DOI: 10.1002/aenm.201301788.

[43] Fan Shi, Lu Li, Xiu-li Wang, Chang-dong Gu, Jiang-ping Tu, Metal oxide/hydroxide based materials for supercapacitors. RSC Adv. 2014;4; 41910-41921, DOI: 10.1039/ C4RA06136E.

[44] Yufei Zhang, Laiquan Li, Haiquan Su, Wei Huang, Xiaochen Dong, Binary metal oxide: advanced energy storage materials in supercapacitors. J. Mater. Chem. A 2015; 3; 43-59, DOI: 10.1039/ C4TA04996A.

[45] Niraj Kumar, P. K. Sahoo, H. S. Panda, Tuning the electro-chemical properties by selectively substituting transition metals on carbon in Ni/Co oxide–carbon composite electrodes for supercapacitor devices. NewJ.Chem. 2017; 41; 3562-3573, DOI: 10.1039/ C6NJ04123J.

[46] Ganesh Kumar Veerasubramani, Karthikeyan Krishnamoorthy, Sang JaeKim, Improved electrochemical performances of binder-free CoMoO$_4$ nanoplate arrays@Ni foam electrode using redox additive electrolyte, J.PowerSources 2016; 306; 378-386, DOI: 10.1016/j.jpowsour.2015.12.034.

[47] Ganesh Kumar Veerasubramani, M. S. P. Sudhakaran, Nagamalleswara Rao Alluri, Karthikeyan Krishnamoorthy, Young Sun Mok, Sang Jae Kim, Effective use of an idle carbon-deposited catalyst for energy storage applications, J. Mater. Chem. A 2016; 4 ;12571-12582, DOI: 10.1039/C6TA05082D.

[48] Ankur Soam, Rahul Kumar, Prasanta Kumar Sahoo, C. Mahender, Balwant Kumar, Nitin Arya, Mamraj Singh, Smrutiranjan Parida, Rajiv O Dusane, Synthesis of Nickel Ferrite Nanoparticles Supported on Graphene Nanosheets as Composite Electrodes for High Performance Supercapacitor, ChemistrySelect 2019; 4; 9952-9958, DOI: 10.1002/slct.201901117.

[49] You Zhou, Zhengyong Huang, Huijun Liao, Jian Li, Hanxiang Wang, Yu Wang, 3D porous graphene/NiCo$_2$O$_4$ hybrid film as an advanced electrode for supercapacitors, Appl. Surf. Sci. 2020;534;147598, DOI: 10.1016/j. apsusc.2020.147598.

[50] Shi Fan, Li Lu, Wang Xiu-li, Gu Chang-dong, Tu Jiang-ping, Metal oxide/hydroxide-based materials for supercapacitors. RSC Adv. 2014; 4; 41910-41921, DOI: 10.1039/c4ra06136e.

[51] Yusin S. I., Bannov A. G., Synthesis of composite electrodes for supercapacitors based on carbon materials and the metal oxide/metal hydroxide system. Protection of Metals and Physical Chemistry of Surfaces. 2017; 53; 475-482, DOI: 10.1134/ S2070205117030261.

[52] Patil U., Lee S. C., Kulkarni S., Sohn J. S., Nam M. S., Han S., Jun S. C., Nanostructured pseudocapacitive materials decorated 3D graphene foam electrodes for next generation supercapacitors. Nanoscale. 2015; 7; 6999-7021, DOI: 10.1039/c5nr01135c.

[53] Yang X., Li J., Hou C., Zhang Q., Li Y., Wang H., Skeleton-Structure WS$_2$@CNT Thin-Film Hybrid Electrodes for High-Performance Quasi-Solid-State Flexible Supercapacitors. Front Chem. 2020; 8; 442, DOI: 10.3389/fchem.2020.00442.

[54] Tang Zhe, Tang Chun-hua, Gong Hao, A High Energy Density Asymmetric Supercapacitor from

Nano-architectured Ni(OH)$_2$/Carbon Nanotube Electrodes. Advanced Functional Materials. 2012; 22; 1272-1278, DOI: 10.1002/adfm.201102796.

[55] Ma Yufang, Chen Wanjun, Zhang Peng, Teng Feng, Zhou Jinyuan, Pan Xiaojun, Xie Erqing, Ni(OH)$_2$ nanosheets grown on a 3D graphene framework as an excellent cathode for flexible supercapacitors. RSC Adv. 2014; 4; 47609-47614, DOI: 10.1039/c4ra08786k.

[56] Jagadale Ajay D., Guan Guoqing, Du Xiao, Hao Xiaogang, Li Xiumin, Abudula Abuliti, Cobalt hydroxide [Co(OH)$_2$] loaded carbon fiber flexible electrode for high performance supercapacitor. RSC Advances. 2015; 5; 56942-56948, DOI: 10.1039/c5ra11366k.

[57] Chen Chao, Cho Misuk, Lee Youngkwan, Electrochemical preparation and energy storage properties of nanoporous Co(OH)$_2$ via pulse current deposition. Journal of Materials Science. 2015; 50; 6491-6497, DOI: 10.1007/s10853-015-9207-6.

[58] Cheng Q., Tang J., Shinya N., Qin L. C., Co(OH)$_2$ nanosheet-decorated graphene-CNT composite for supercapacitors of high energy density. Sci Technol Adv Mater. 2014; 15; 014206, DOI: 10.1088/1468-6996/15/1/014206.

[59] Zhang Jing, Wang Xiuchun, Ma Jie, Liu Shuo, Yi Xibin, Preparation of cobalt hydroxide nanosheets on carbon nanotubes/carbon paper conductive substrate for supercapacitor application. Electrochimica Acta. 2013; 104 110-116, DOI: 10.1016/j.electacta.2013.04.052.

[60] Chen Li-Feng, Yu Zi-You, Wang Jia-Jun, Li Qun-Xiang, Tan Zi-Qi, Zhu Yan-Wu, Yu Shu-Hong, Metal-like fluorine-doped β-FeOOH nanorods grown on carbon cloth for scalable high-performance supercapacitors.

Nano Energy. 2015; 11; 119-128, DOI: 10.1016/j.nanoen.2014.10.005.

[61] Owusu K. A., Qu L., Li J., Wang Z., Zhao K., Yang C., Hercule K. M., Lin C., Shi C., Wei Q., Zhou L., Mai L., Low-crystalline iron oxide hydroxide nanoparticle anode for high-performance supercapacitors. Nat Commun. 2017; 8; 14264, DOI: 10.1038/ncomms14264.

[62] Shen Baoshou, Guo Ruisheng, Lang Junwei, Liu Li, Liu Lingyang, Yan Xingbin, A high-temperature flexible supercapacitor based on pseudocapacitive behavior of FeOOH in an ionic liquid electrolyte. Journal of Materials Chemistry A. 2016; 4; 8316-8327, DOI: 10.1039/c6ta01734g.

[63] Sun C., Pan W., Zheng D., Zheng Y., Zhu J., Liu C., Low-Crystalline FeOOH Nanoflower Assembled Mesoporous Film Anchored on MWCNTs for High-Performance Supercapacitor Electrodes. ACS Omega. 2020; 5; 4532-4541, DOI: 10.1021/acsomega.9b03869.

[64] Liu Jiaqi, Zheng Mingbo, Shi Xiaoqin, Zeng Haibo, Xia Hui, Amorphous FeOOH Quantum Dots Assembled Mesoporous Film Anchored on Graphene Nanosheets with Superior Electrochemical Performance for Supercapacitors. Advanced Functional Materials. 2016; 26; 919-930, DOI: 10.1002/adfm.201504019.

[65] Wei Y., Ding R., Zhang C., Lv B., Wang Y., Chen C., Wang X., Xu J., Yang Y., Li Y., Facile synthesis of self-assembled ultrathin alpha-FeOOH nanorod/graphene oxide composites for supercapacitors. J Colloid Interface Sci. 2017; 504; 593-602, DOI: 10.1016/j.jcis.2017.05.112.

[66] Wang Fuxin, Zeng Yinxiang, Zheng Dezhou, Li Cheng, Liu Peng, Lu Xihong, Tong Yexiang, Three-dimensional iron oxyhydroxide/reduced graphene oxide composites as advanced electrode for

electrochemical energy storage. Carbon. 2016; 103; 56-62, DOI: 10.1016/j. carbon.2016.02.088.

[67] Li Xiao, Zhu Hongwei, Two-dimensional MoS_2: Properties, preparation, and applications. Journal of Materiomics. 2015; 1; 33-44, DOI: 10.1016/j.jmat.2015.03.003.

[68] Li Ming-Yang, Chen Chang-Hsiao, Shi Yumeng, Li Lain-Jong, Heterostructures based on two-dimensional layered materials and their potential applications. Materials Today. 2016; 19; 322-335, DOI: 10.1016/j. mattod.2015.11.003.

[69] Ge Yu, Jalili Rouhollah, Wang Caiyun, Zheng Tian, Chao Yunfeng, Wallace Gordon G., A robust free-standing MoS_2/poly(3,4-ethylenedio xythiophene):poly(styrenesulfonate) film for supercapacitor applications. Electrochimica Acta. 2017; 235; 348-355, DOI: 10.1016/j.electacta.2017.03.069.

[70] Soon Jia Mei, Loh Kian Ping, Electrochemical Double-Layer Capacitance of MoS_2 Nanowall Films. Electrochemical and Solid State Letters. 2007; 10; A250-A254, DOI: 10.1149/1.2778851兴.

[71] Huang Ke-Jing, Wang Lan, Zhang Ji-Zong, Wang Ling-Ling, Mo Yan-Ping, One-step preparation of layered molybdenum disulfide/multi-walled carbon nanotube composites for enhanced performance supercapacitor. Energy. 2014; 67; 234-240, DOI: 10.1016/j.energy.2013.12.051.

[72] Ali Gomaa A. M., Thalji Mohammad R., Soh Wee Chen, Algarni H., Chong Kwok Feng, One-step electrochemical synthesis of MoS_2/graphene composite for supercapacitor application. Journal of Solid State Electrochemistry. 2020; 24; 25-34, DOI: 10.1007/s10008-019-04449-5.

[73] Ali B. A., Metwalli O. I., Khalil A. S. G., Allam N. K., Unveiling the Effect of the Structure of Carbon Material on the Charge Storage Mechanism in MoS_2-Based Supercapacitors. ACS Omega. 2018; 3; 16301-16308, DOI: 10.1021/acsomega.8b02261.

[74] Sun G., Zhang X., Lin R., Yang J., Zhang H., Chen P., Hybrid fibers made of molybdenum disulfide, reduced graphene oxide, and multi-walled carbon nanotubes for solid-state, flexible, asymmetric supercapacitors. Angew Chem Int Ed Engl. 2015; 54; 4651-4656, DOI: 10.1002/anie.201411533.

[75] Zhang Y., He T., Liu G., Zu L., Yang J., One-pot mass preparation of MoS_2/C aerogels for high-performance supercapacitors and lithium-ion batteries. Nanoscale. 2017; 9; 10059-10066, DOI: 10.1039/c7nr03187d.

[76] Sun Tianhua, Li Zhangpeng, Liu Xiaohong, Ma Limin, Wang Jinqing, Yang Shengrong, Facile construction of 3D graphene/MoS_2 composites as advanced electrode materials for supercapacitors. Journal of Power Sources. 2016; 331; 180-188, DOI: 10.1016/j.jpowsour.2016.09.036.

[77] Shang Xiao, Chi Jing-Qi, Lu Shan-Shan, Gou Jian-Xia, Dong Bin, Li Xiao, Liu Yan-Ru, Yan Kai-Li, Chai Yong-Ming, Liu Chen-Guang, Carbon fiber cloth supported interwoven WS_2 nanosplates with highly enhanced performances for supercapacitors. Applied Surface Science. 2017; 392; 708-714, DOI: 10.1016/j.apsusc.2016.09.058.

[78] Xu Yunpeng, Wang Lizhong, Xu Qiang, Liu Liyun, Fang Xiaochen, Shi Ce, Ye Bin, Chen Lingyun, Peng Wenyi, Liu Zongjian, Chen Weifan, 3D hybrids based on WS_2/N, S co-doped reduced graphene oxide: Facile fabrication and superior performance in supercapacitors. Applied Surface Science. 2019; 480; 1126-1135, DOI: 10.1016/j.apsusc.2019.02.217.

[79] Ma Lin, Xu Limei, Zhou Xiaoping, Xu Xuyao, Zhang Lingling, Synthesis of a hierarchical MoSe$_2$/C hybrid with enhanced electrochemical performance for supercapacitors. RSC Advances. 2016; 6; 91621-91628, DOI: 10.1039/c6ra16157j.

[80] Liu Y., Li W., Chang X., Chen H., Zheng X., Bai J., Ren Z., MoSe$_2$ nanoflakes-decorated vertically aligned carbon nanotube film on nickel foam as a binder-free supercapacitor electrode with high rate capability. J Colloid Interface Sci. 2020; 562; 483-492, DOI: 10.1016/j.jcis.2019.11.089.

[81] Kirubasankar Balakrishnan, Vijayan Shobana, Angaiah Subramania, Sonochemical synthesis of a 2D–2D MoSe$_2$/graphene nanohybrid electrode material for asymmetric supercapacitors. Sustainable Energy & Fuels. 2019; 3; 467-477, DOI: 10.1039/c8se00446c.

[82] Huang Ke-Jing, Zhang Ji-Zong, Cai Jia-Lin, Preparation of porous layered molybdenum selenide-graphene composites on Ni foam for high-performance supercapacitor and electrochemical sensing. Electrochimica Acta. 2015; 180; 770-777, DOI: 10.1016/j.electacta.2015.09.016.

[83] Wei S., Wan C., Jiao Y., Li X., Li J., Wu Y., 3D nanoflower-like MoSe$_2$ encapsulated with hierarchically anisotropic carbon architecture: a new and free-standing anode with ultra-high areal capacitance for asymmetric supercapacitors. Chem Commun (Camb). 2020; 56; 340-343, DOI: 10.1039/c9cc07362k.